Supporting Information for

Light- and Temperature-Assisted Spin State Annealing: Accessing the Hidden Multistability

Yan-Cong Chen, Yan Meng, Yan-Jie Dong, Xiao-Wei Song, Guo-Zhang Huang, Chuan-Lei Zhang, Zhao-Ping Ni, Jakub Navařík, Ondřej Malina, Radek Zbořil and Ming-Liang Tong

CONTENTS

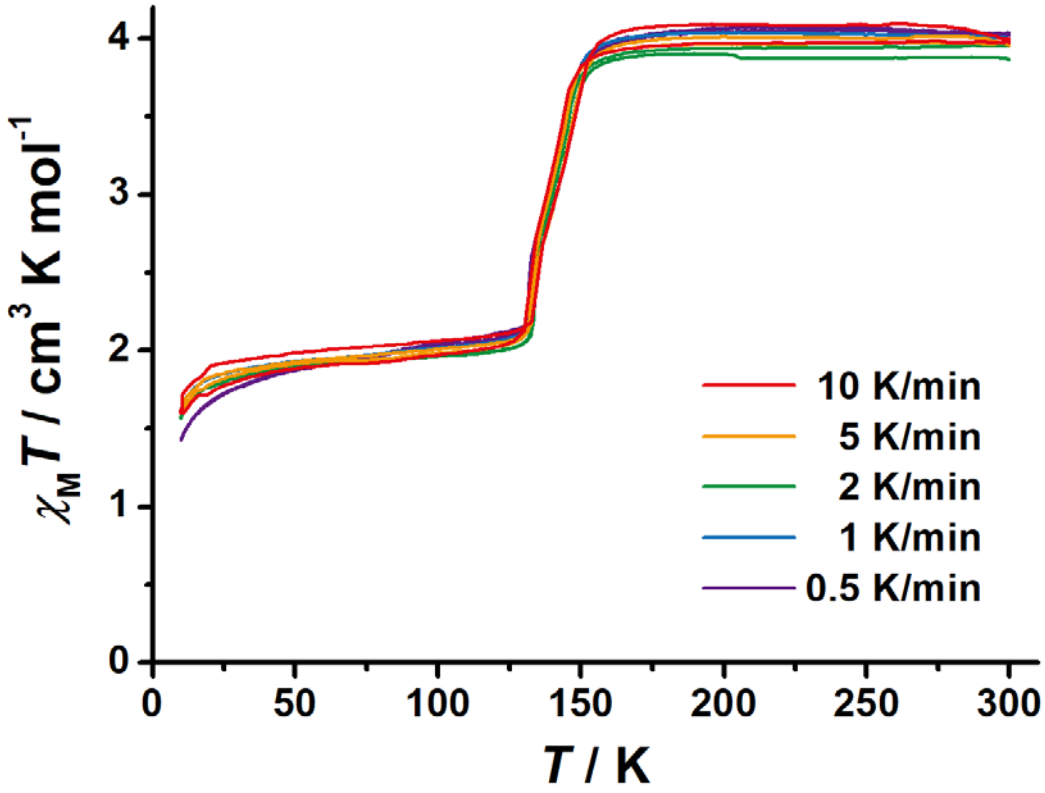

Figure S1 Temperature dependence of the molar magnetic susceptibility $\chi_M T$ products for **1** in different temperature sweeping rates.

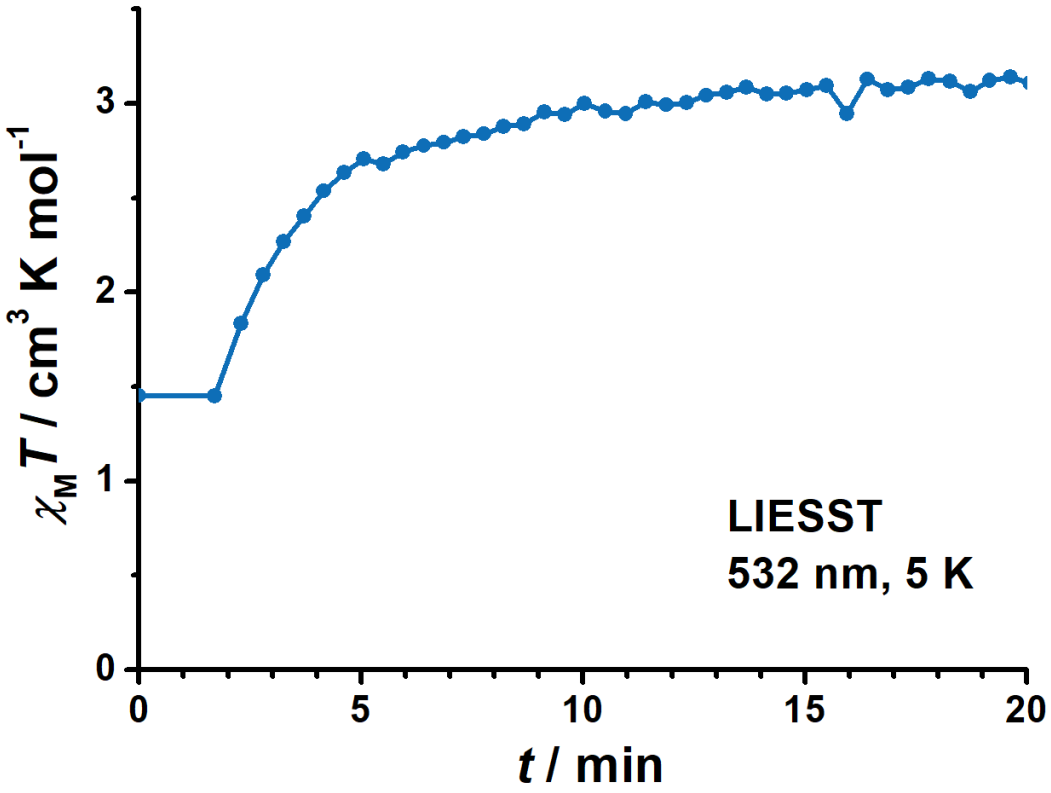

Figure S2 Time dependence of the molar magnetic susceptibility $\chi_M T$ products for **1** during LIESST (from MS to HS state) at 5 K. The laser was turned on immediately after t = 0.

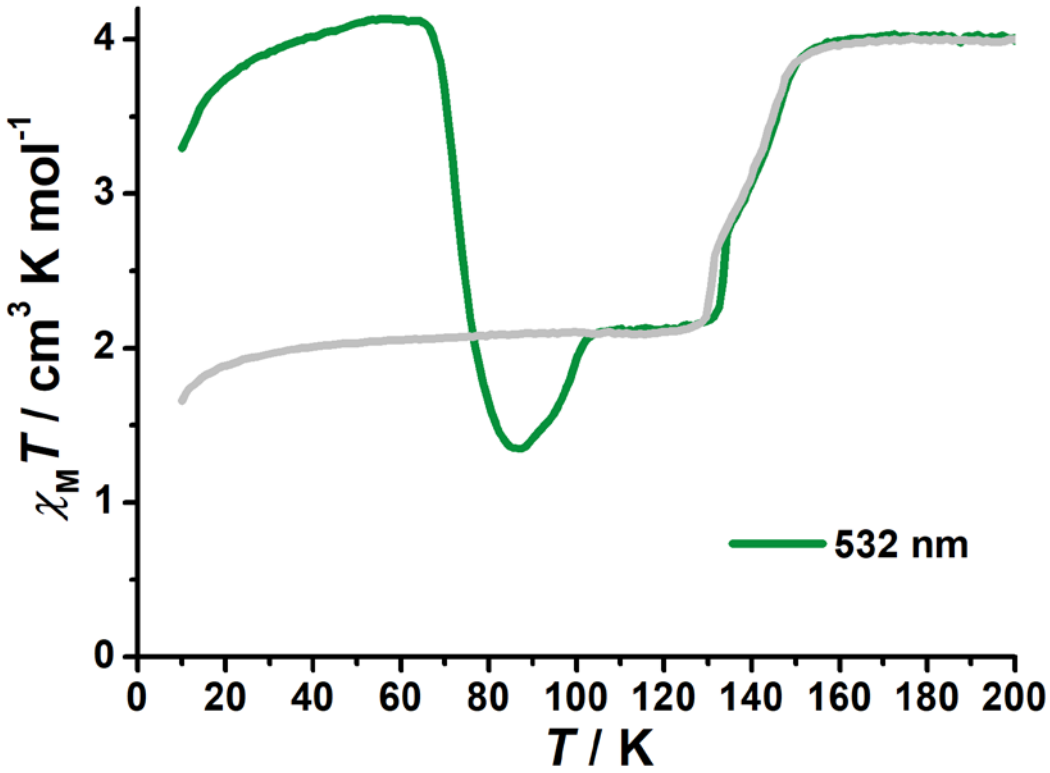

Figure S3 Temperature dependence of $\chi_M T$ for **1** in warming mode after LIESST at 5 K, without holding or annealing. The grey line represents the normal SCO in the cooling mode for reference. Temperature sweeping rate: 2 K/min.

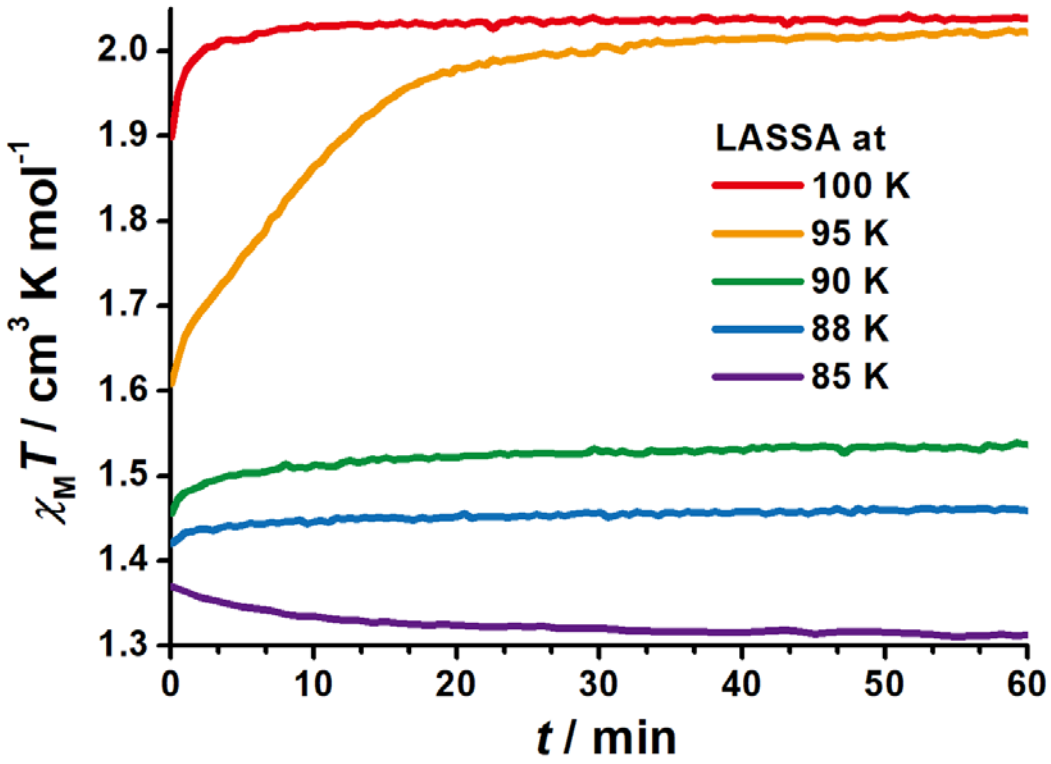

Figure S4 Time dependence of the molar magnetic susceptibility $\chi_M T$ products for **1** during high temperature LASSA: LIESST from MS to HS state at 5 K and then annealed at various temperatures.

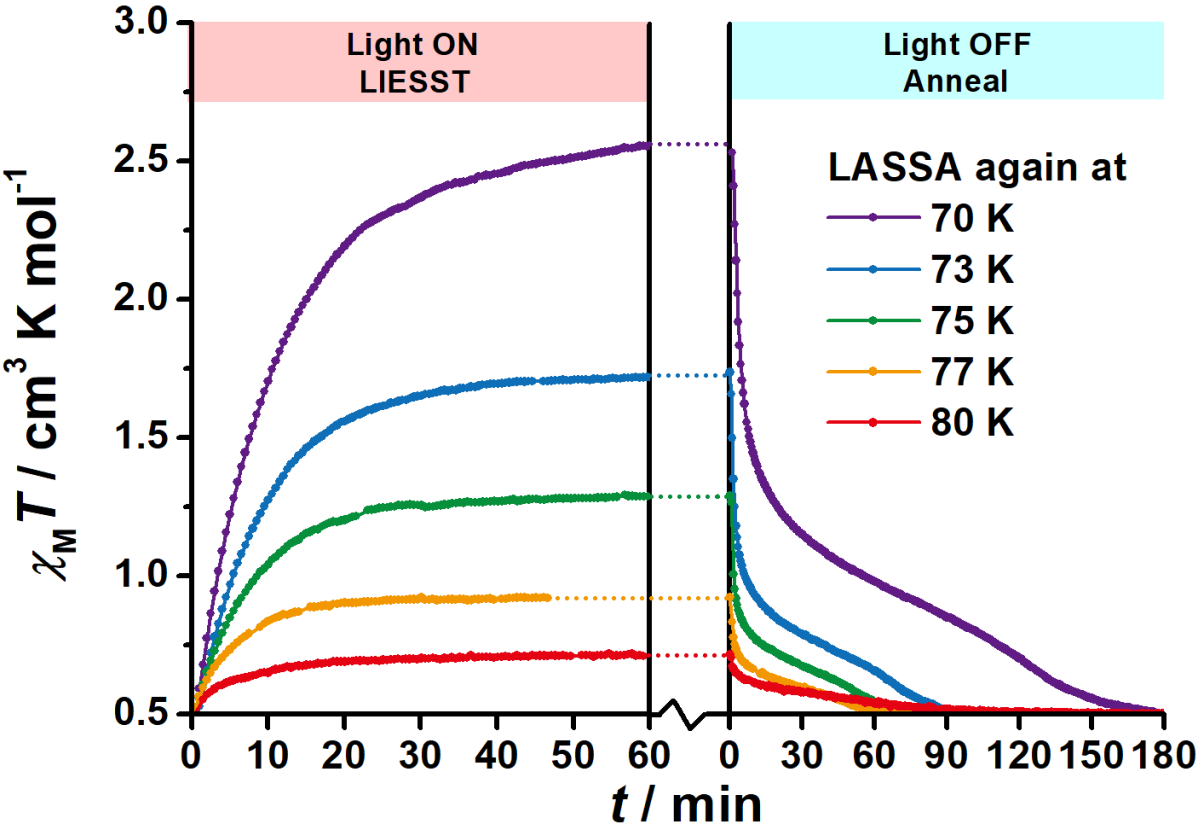

Figure S5 Time dependence of the molar magnetic susceptibility $\chi_M T$ products for **1** starting from the LASSA-LS state obtained at 75 K, and performing LASSA again at various temperatures with a 532 nm laser.

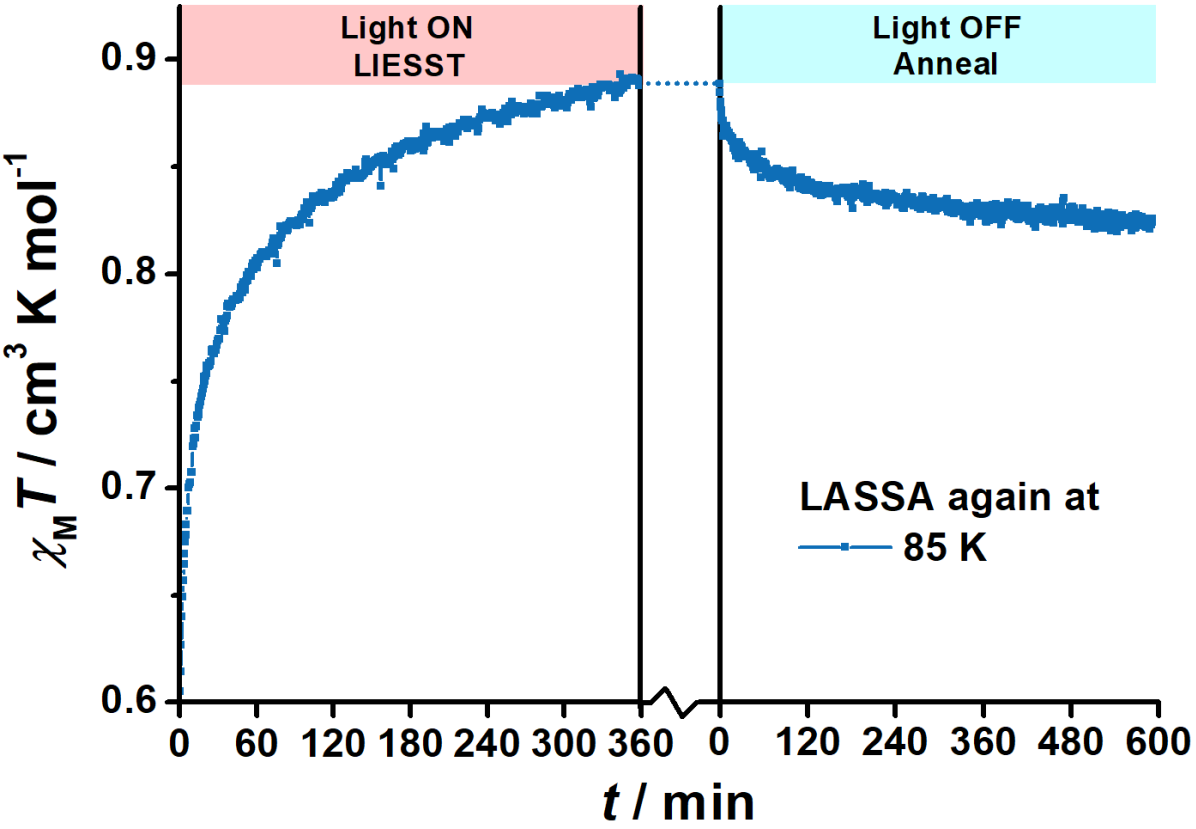

Figure S6 Time dependence of the molar magnetic susceptibility $\chi_M T$ products for **1** starting from the LASSA-LS state obtained at 75 K, and performing LASSA again at 85 K with a 532 nm laser. Note the largely different time scale with Figure S5.

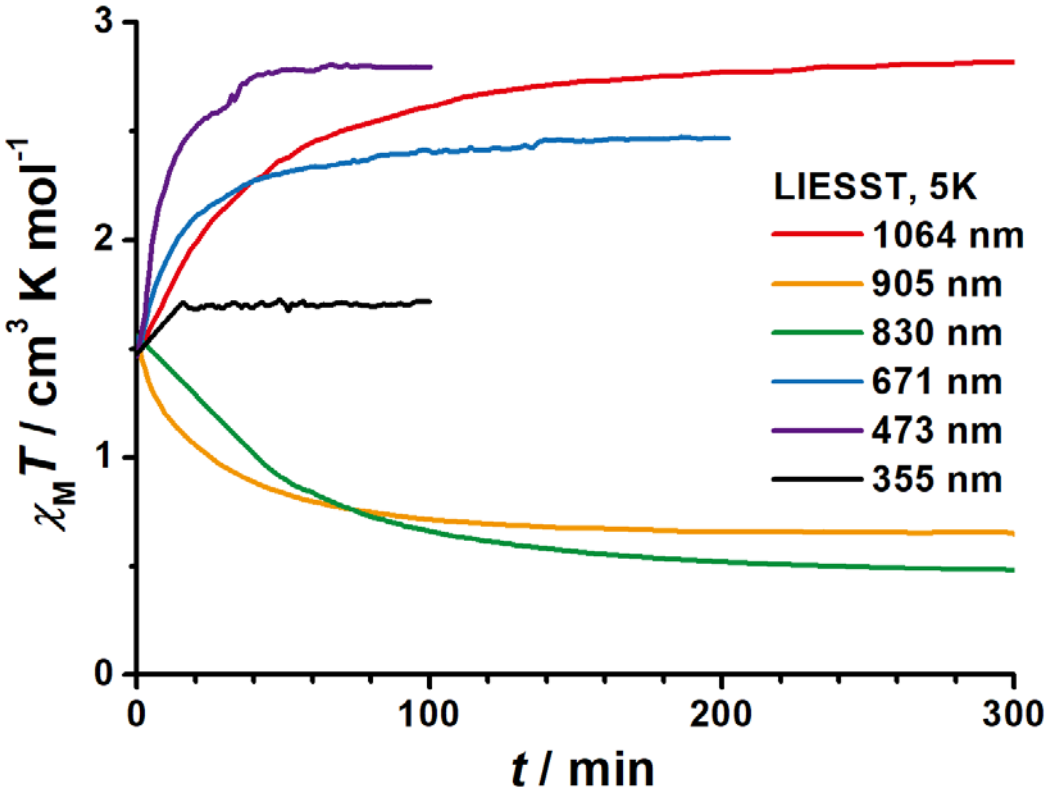

Figure S7 Time dependence of the molar magnetic susceptibility $\chi_M T$ products for **1** during LIESST (from MS state) at 5 K with various sources of laser until saturation. The laser was turned on immediately after t = 0.

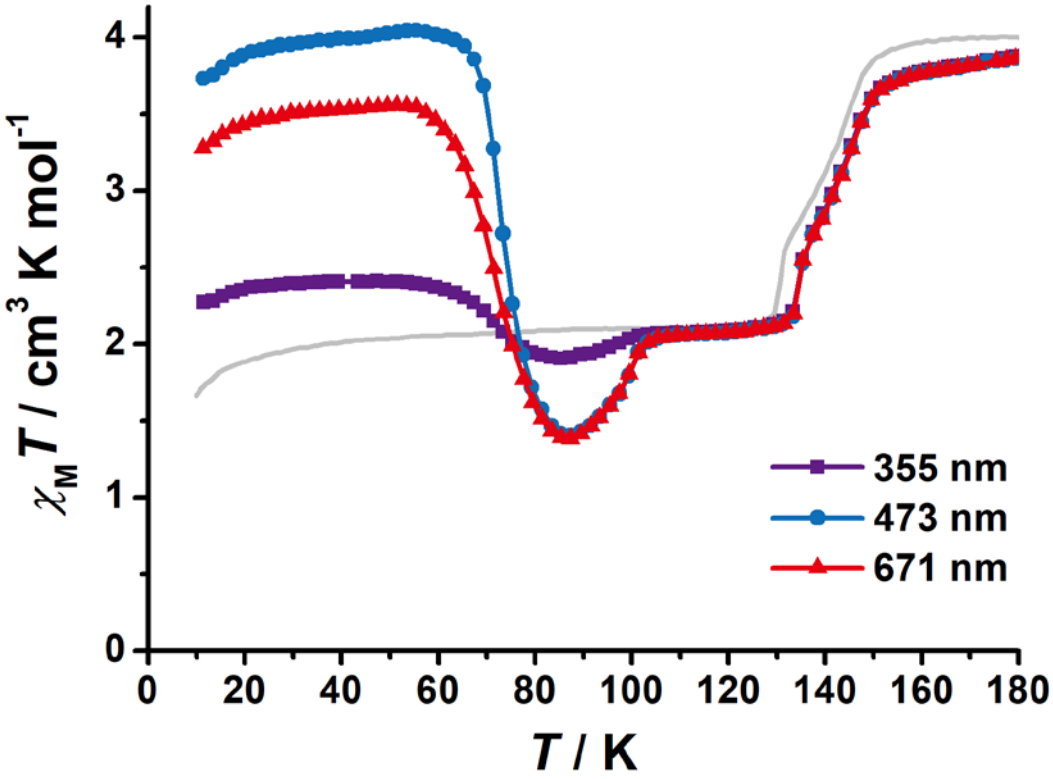

Figure S8 Temperature dependence of the molar magnetic susceptibility $\chi_M T$ products for **1** in warming mode after LIESST (from MS state at 5 K) with a 355 nm (purple), 473 nm (blue) and 671 nm (red) laser. The grey line represents the normal SCO in the cooling mode for reference. Temperature sweeping rate: 2 K/min.

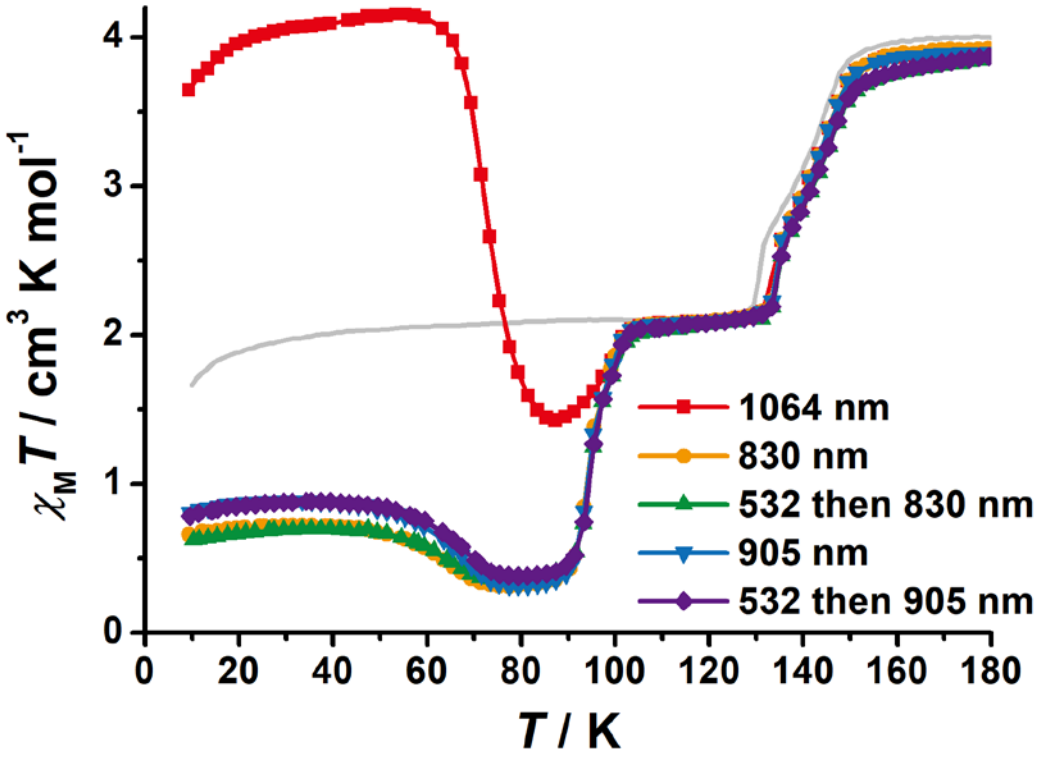

Figure S9 Temperature dependence of the molar magnetic susceptibility $\chi_M T$ products for **1** in warming mode after LIESST (from MS state at 5 K) with a infrared 1064 nm (red), 830 nm (orange) and 905 nm (blue) laser, and after bidirectional LIESST with firstly a 532 nm laser (which excites **1** from MS to HS state at 5 K) and secondly a 830 nm (green) or 905 nm laser (purple). The grey line represents the normal SCO in the cooling mode for reference. Temperature sweeping rate: 2 K/min.

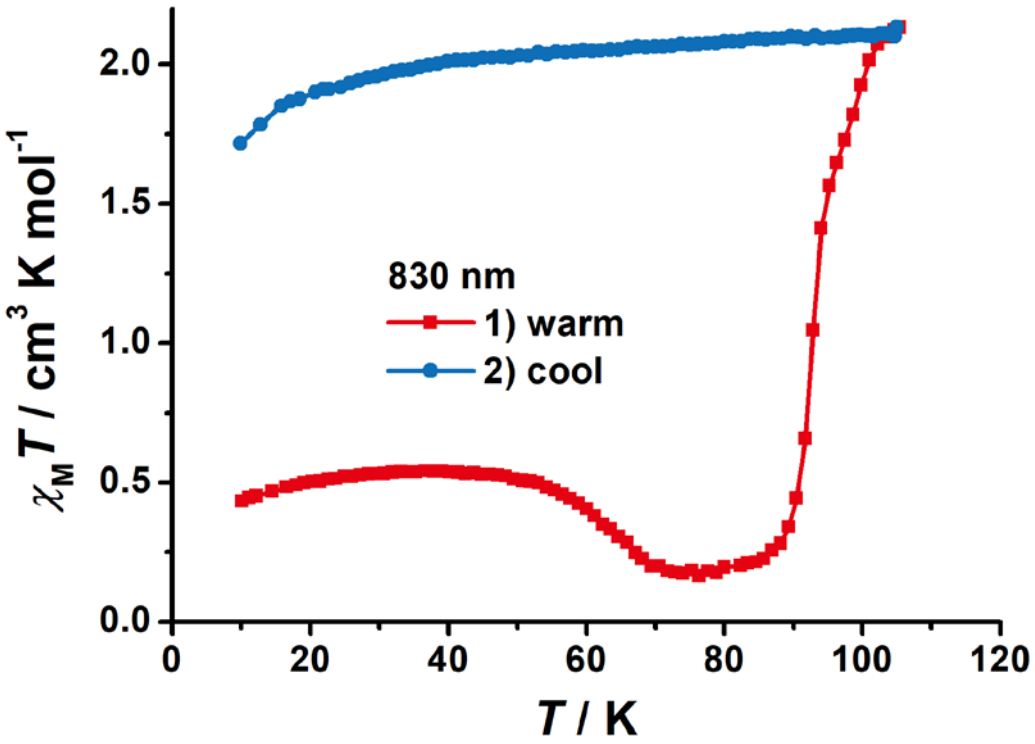

Figure S10 Temperature dependence of the molar magnetic susceptibility $\chi_M T$ products for **1** after the 830 nm reverse-LIESST (from MS state at 5 K) in warming mode to 105 K (red) and then in cooling (blue) mode. No hidden hysteresis is observed. Temperature sweeping rate: 2 K/min.

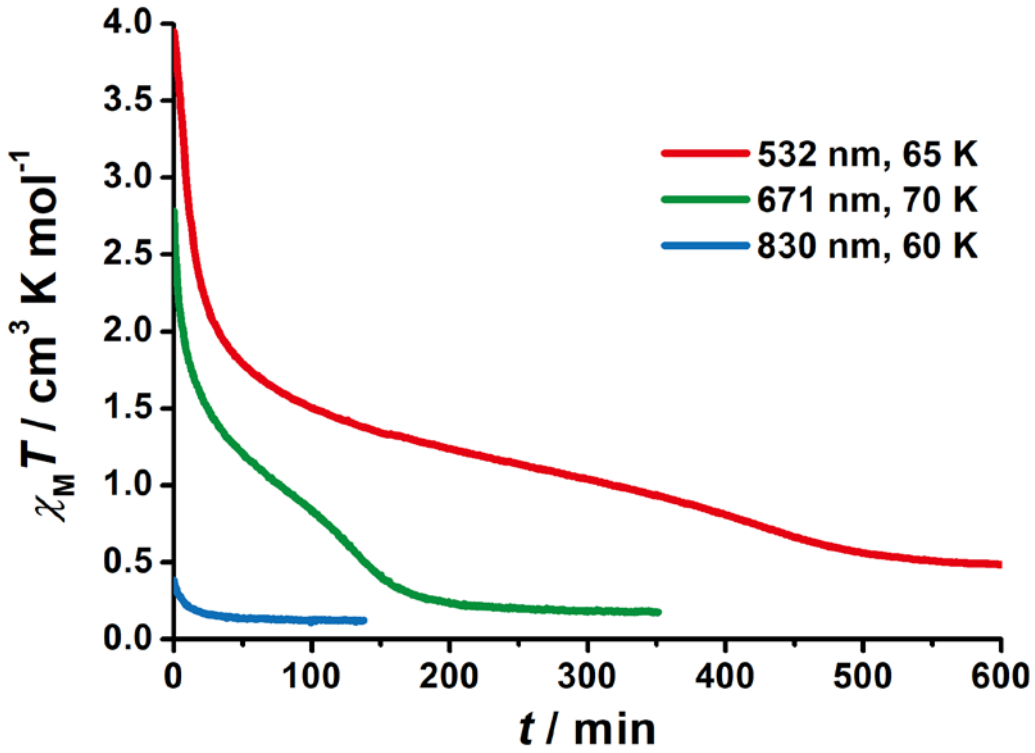

Figure S11 Time dependence of the molar magnetic susceptibility $\chi_M T$ products for **1** after LIESST with various lasers and then annealing at indicated temperatures.

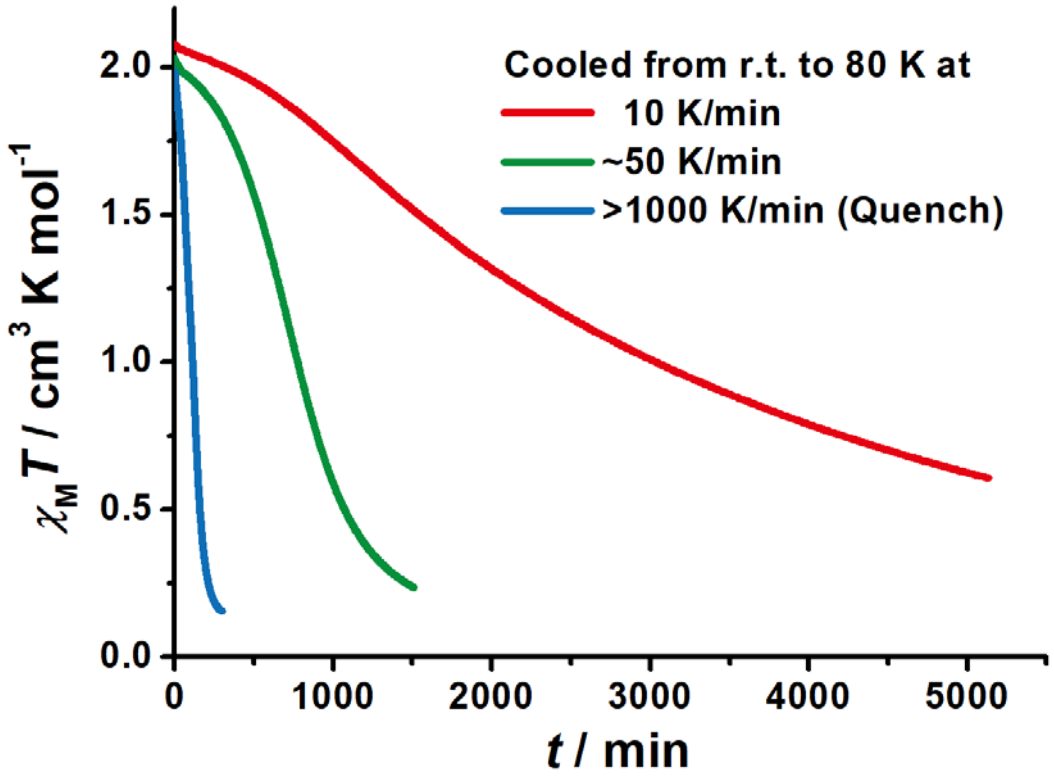

Figure S12 Time dependence of the molar magnetic susceptibility $\chi_M T$ products for **1** after cooling from room temperature to 80 K at various cooling rates.

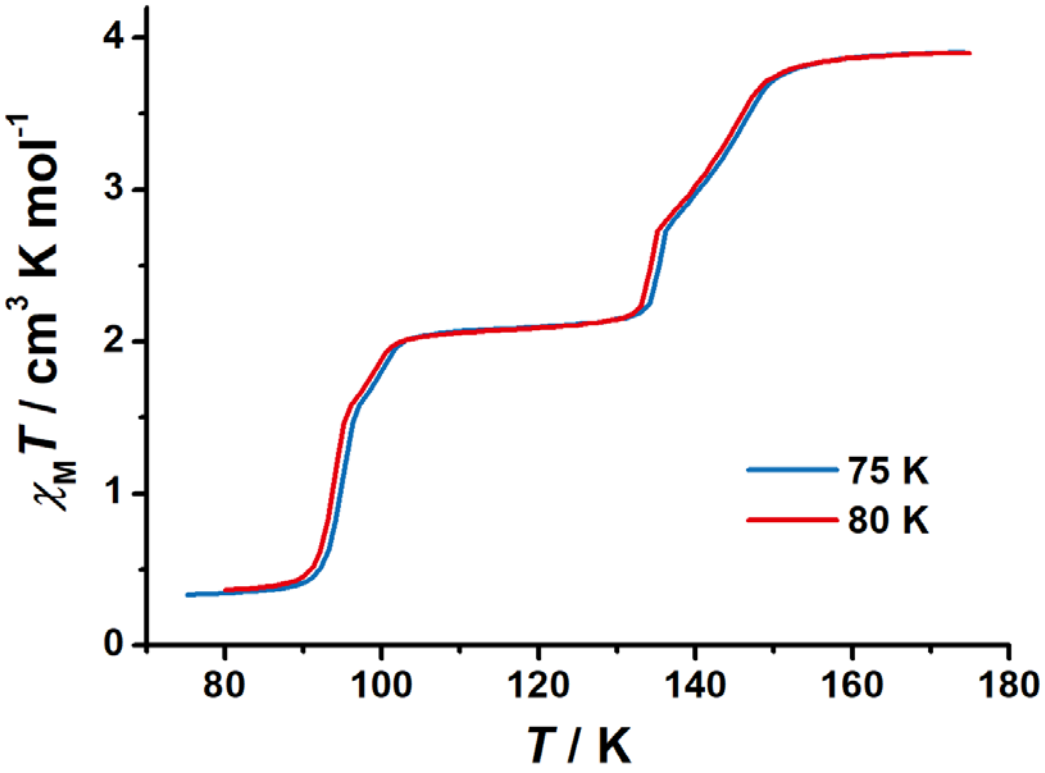

Figure S13 Temperature dependence of the molar magnetic susceptibility $\chi_M T$ products for **1** in warming mode starting from the TASSA-LS states obtained at 75 K (blue) and 80 K (red). Temperature sweeping rate: 2 K/min.

Table S1. Crystal Data and Structural Refinements for **1**.

State	**170HS**	**80MS-Order**	**80MS-Disorder**	**80LS**
Chemical formula		$C_{22}H_{14}Au_2FeN_6$		
Formula Mass		812.17		
Radiation type		$Mo_{K\alpha}$		
No. of formula units per unit cell, Z		4		
$F(000)$		1488		
Temperature / K	170(2)	80(2)	80(2)	80(2)
Crystal system	Monoclinic	Triclinic	Monoclinic	Monoclinic
Space group	$P2_1/c$	$P\bar{1}$	$P2_1/c$	$P2_1/c$
a / Å	10.8116(5)	10.7701(10)	10.7397(12)	10.7739(5)
b / Å	14.4381(6)	14.1621(12)	14.1109(14)	13.9861(6)
c / Å	14.9803(7)	14.7425(13)	14.6790(16)	14.5762(7)
α / °	90	90.082(3)	90	90
β / °	96.596(2)	96.077(3)	95.980(3)	95.770(2)
γ / °	90	90.471(3)	90	90
Unit cell volume / Å^3	2322.93(18)	2235.9(3)	2212.5(4)	2185.28(17)
Absorption coefficient, μ / mm^{-1}	13.237	13.752	13.898	14.070
No. of reflections measured	74552	62051	14510	66879
No. of independent reflections	4815	7641	4432	4532
R_{int}	0.0383	0.0452	0.0887	0.0462
R_1 [a] ($I > 2\sigma(I)$)	0.0301	0.0909	0.0676	0.0391
wR_2 [b] (all data)	0.0745	0.2285	0.1487	0.0865
Goodness of fit on F^2	1.077	1.349	1.107	1.162

[a] $R_1 = \Sigma||F_o| - |F_c||/\Sigma|F_o|$

[b] $wR_2 = [\Sigma w(F_o^2 - F_c^2)^2/\Sigma w(F_o^2)^2]^{1/2}$.

Table S2. Selected bond lengths (Å) and bond angles (°), sorted in ascending order, for **1**.

	170HS	80MS-Order		80MS-Disorder	80LS
		Fe1	Fe2		
Fe-N	2.145(5)	2.07(2)	1.97(2)	2.015(16)	1.974(8)
	2.159(5)	2.10(2)	1.97(3)	2.028(17)	1.976(9)
	2.165(5)	2.11(2)	1.97(3)	2.039(17)	1.981(8)
	2.168(5)	2.13(3)	2.00(2)	2.044(17)	1.985(9)
	2.198(6)	2.15(3)	2.05(2)	2.072(13)	2.041(8)
	2.200(5)	2.16(2)	2.05(2)	2.080(16)	2.044(9)
N-Fe-N	88.20(19)	87.4(9)	88.4(9)	88.2(6)	88.1(3)
	88.21(19)	88.4(9)	88.6(10)	88.7(6)	88.6(3)
	88.9(2)	88.4(9)	88.8(10)	88.8(6)	88.7(3)
	89.1(2)	88.5(9)	89.2(10)	89.3(6)	89.6(3)
	89.4(2)	89.5(9)	89.3(9)	89.4(6)	89.6(3)
	89.6(2)	89.5(9)	89.6(10)	89.7(6)	89.8(3)
	90.2(2)	90.6(10)	89.7(9)	89.7(6)	90.1(3)
	90.3(2)	90.7(9)	90.1(10)	89.7(6)	90.3(3)
	90.7(2)	90.7(9)	91.1(10)	90.6(6)	90.5(3)
	90.7(2)	91.2(9)	91.5(10)	91.1(6)	91.2(3)
	92.0(2)	91.4(10)	91.5(10)	92.1(6)	91.5(3)
	92.6(2)	93.6(9)	92.3(10)	92.6(6)	92.0(3)

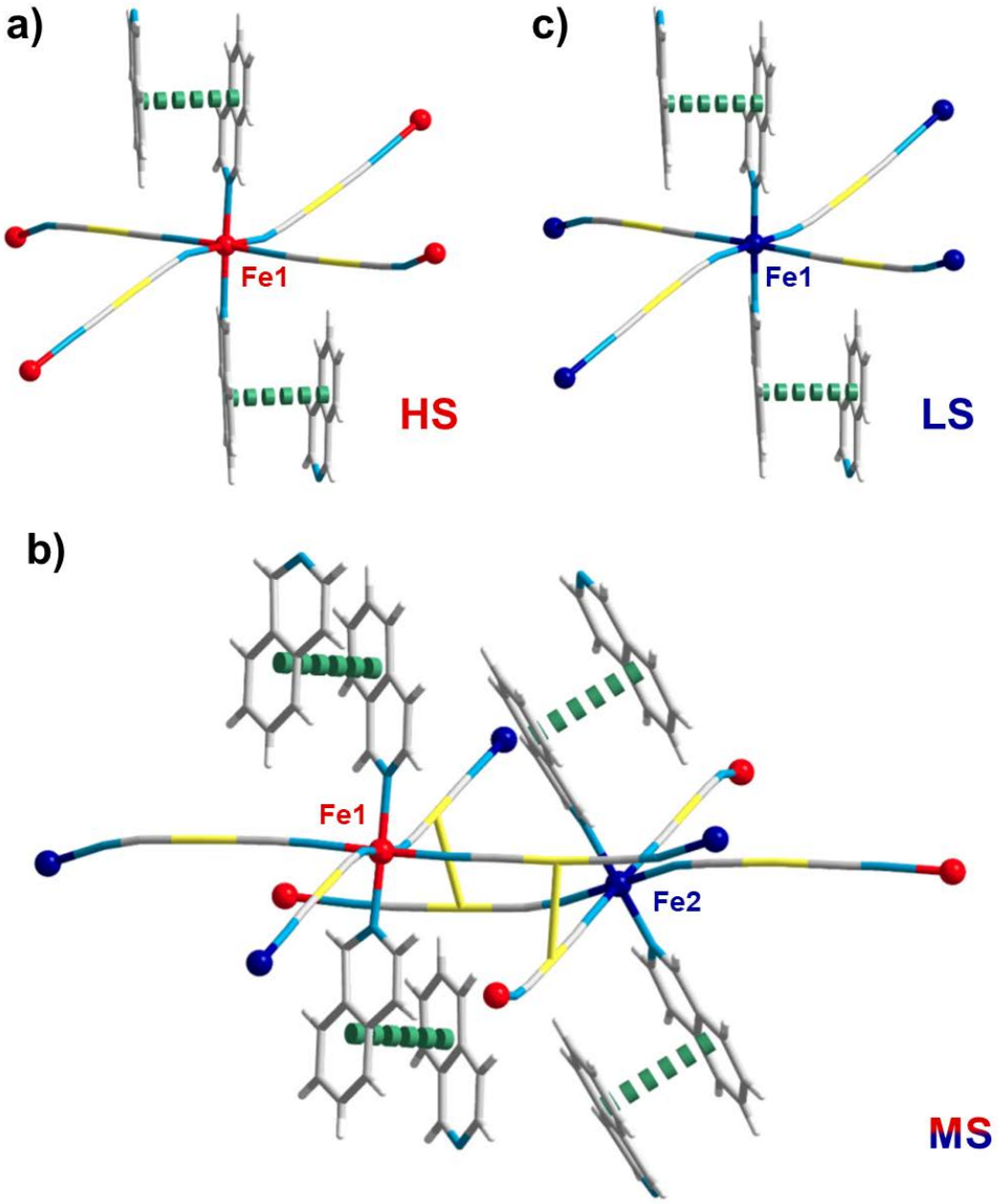

Figure S14. Crystal structure for **1** in the HS state at 170 K (a); in the ordered MS state at 80 K (b, by slow cooling); and in the LS state at 80 K (c, by rapid quench and annealed), showing the coordination environment of Fe, the spin state of the neighboring Fe (by color), and the interlayer offset π-π stacking (green dash lines). Color codes: Fe(HS), red; Fe(LS), blue; Au, yellow; N, cyan; C, gray.

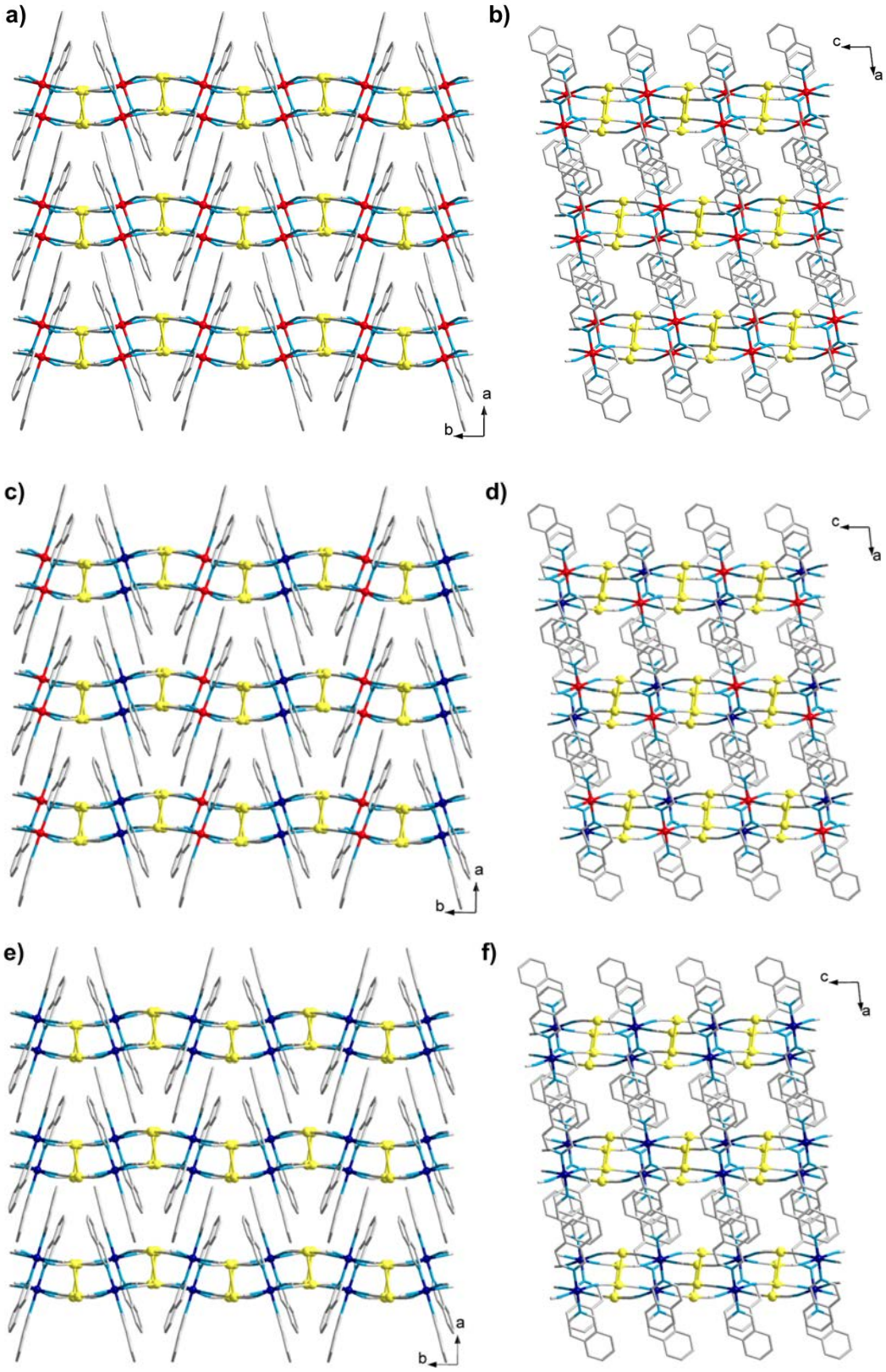

Figure S15. Crystal structure for **1** in the HS state at 170 K (a-b); in the ordered MS state at 80 K (c-d, by slow cooling); and in the LS state at 80 K (e-f, by rapid quench and annealed), showing the packing diagram along the *c* axis (a, c, e) and the *b* axis (b,d,f). Color codes: Fe(HS), red; Fe(LS), blue; Au, yellow; N, cyan; C, gray.

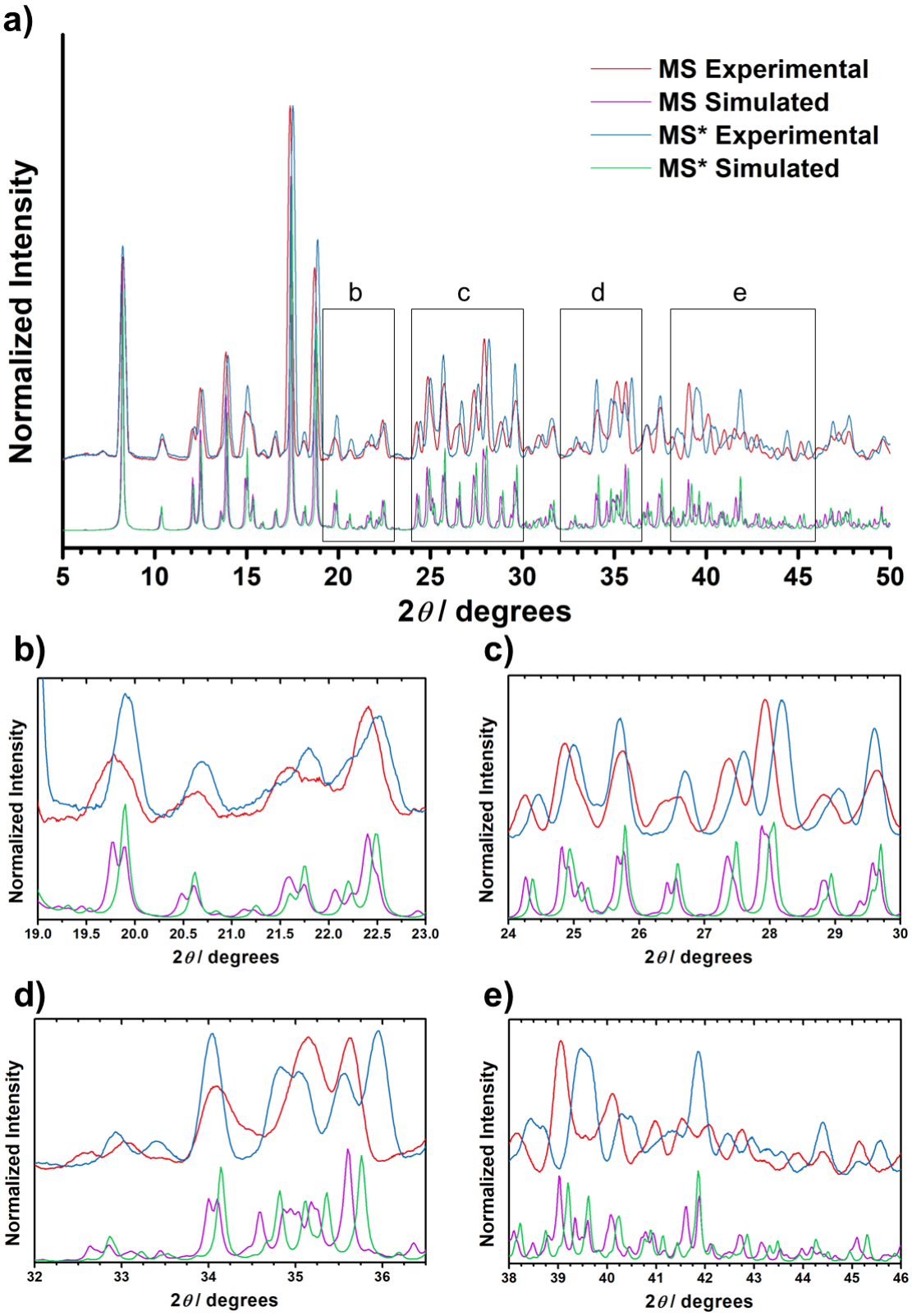

Figure S16. Powder XRD patterns for **1** at 80 K in the MS state (red) and the MS* state (blue), compared with the simulated patterns (purple, and green, respectively) from the crystal structure.

Table S3. Selected structural parameters in different states for **1**.

	170HS	**80MS-Order**	**80MS-Disorder**	**80LS**
Fe…(NCAuCN)…Fe[a]/Å	10.3975(11) 10.4080(11)	10.202(6) 10.225(6) 10.226(6) 10.232(6)	10.174(4) 10.188(4)	10.0914(19) 10.1096(19)
Fe…Fe[b]/Å	7.6570(12)	7.5329(45)	7.503(4)	7.4549(19)
Au…Au[c]/Å	3.0490(3)	3.0182(15) 3.0187(15)	3.0037(9)	2.9985(5)
π…π[d]/Å	3.5309(1)	3.4833(3) 3.4871(3)	3.4698(3)	3.4409(1)

[a]The Fe…Fe distance linked by $[Au(CN)_2]^-$

[b]The nearest Fe…Fe distance.

[c]The aurophilic interactions.

[d]The interlayer offset π-π stacking between isoq ligands (as depicted in Figure S14).

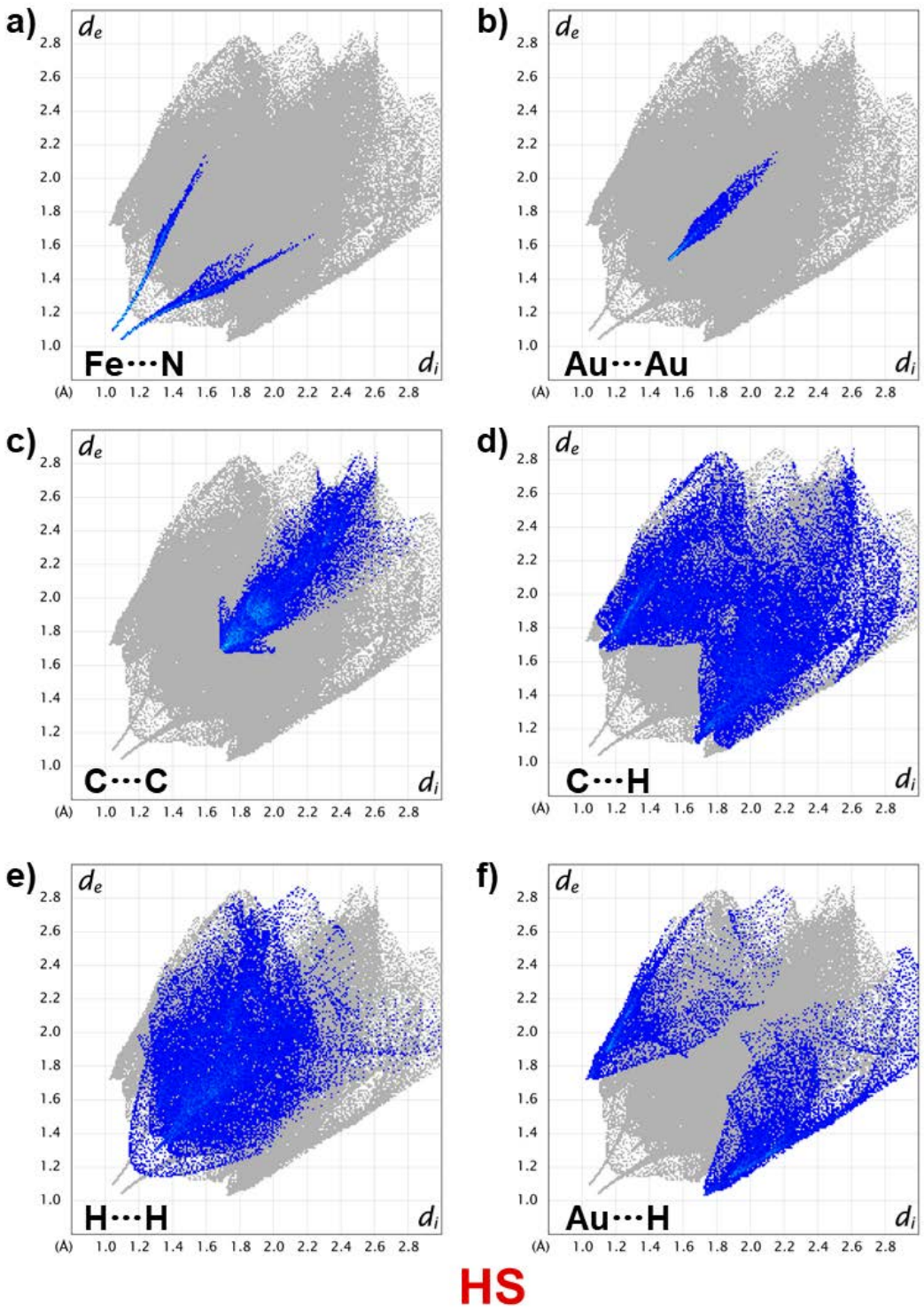

Figure S17. Fingerprint plot of **1** in the HS state at 170 K resolved into Fe...N (a), Au…Au (b), C…C (c), C…H (d) H…H (e) and Au…H (f) contacts. The full fingerprint is plotted beneath (grey).

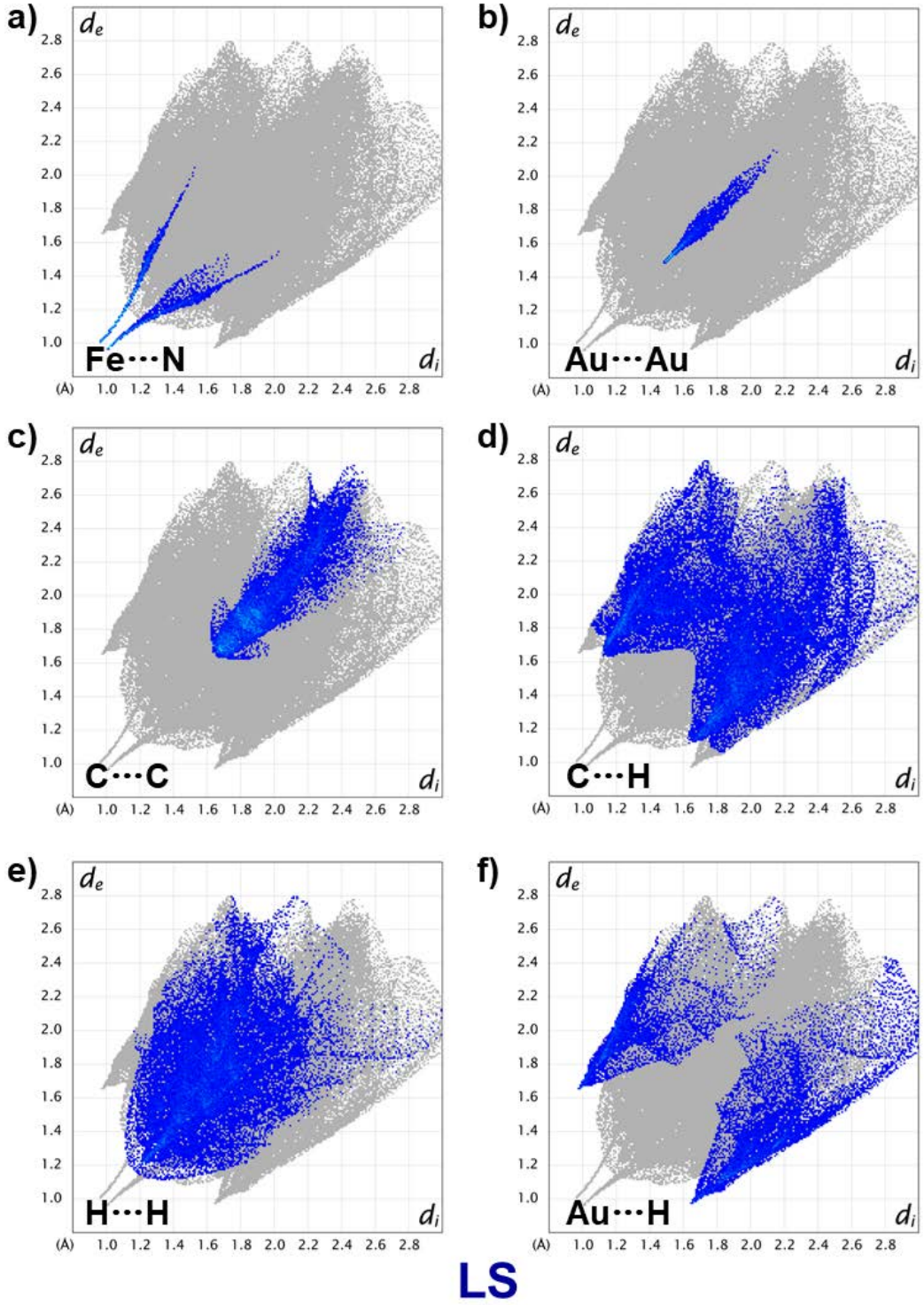

Figure S18. Fingerprint plot of **1** in the LS state at 80 K resolved into Fe...N (a), Au…Au (b), C…C (c), C…H (d) H…H (e) and Au…H (f) contacts. The full fingerprint is plotted beneath (grey).

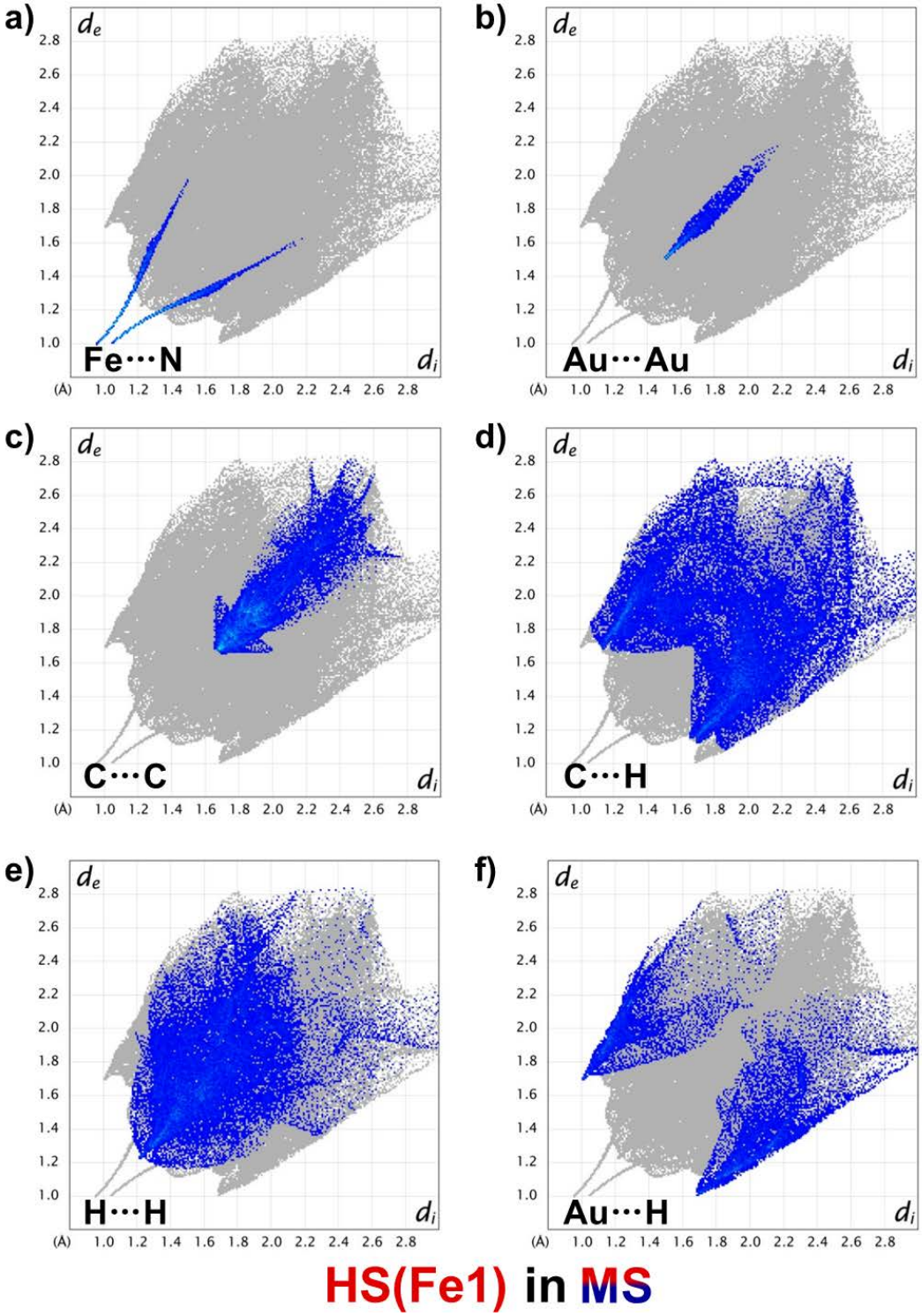

Figure S19. Fingerprint plot of the high spin Fe1 in **1** in the ordered MS state at 80 K resolved into Fe...N (a), Au…Au (b), C…C (c), C…H (d) H…H (e) and Au…H (f) contacts. The full fingerprint is plotted beneath (grey).

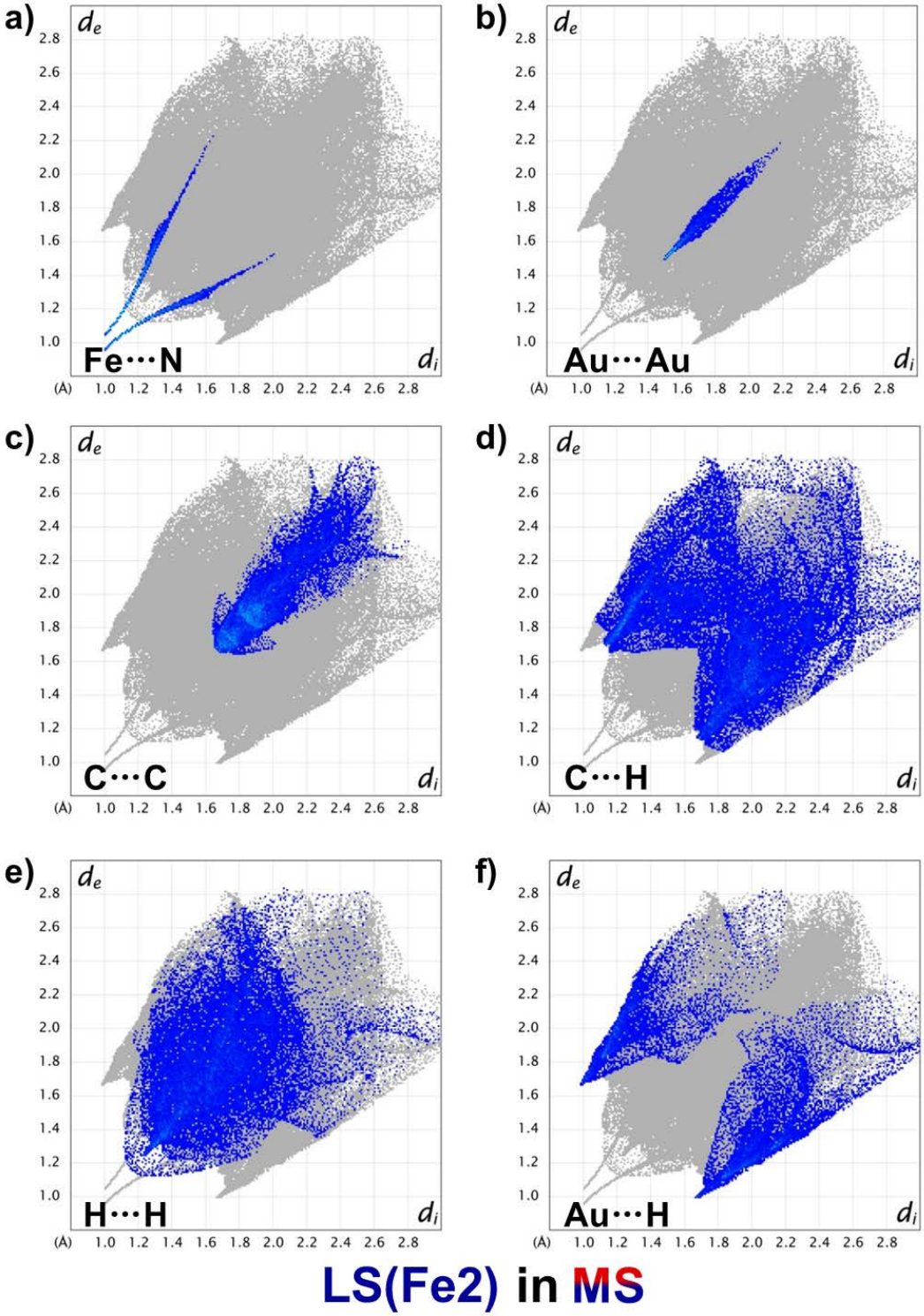

Figure S20. Fingerprint plot of the low spin Fe2 in **1** in the ordered MS state at 80 K resolved into Fe...N (a), Au…Au (b), C…C (c), C…H (d) H…H (e) and Au…H (f) contacts. The full fingerprint is plotted beneath (grey).

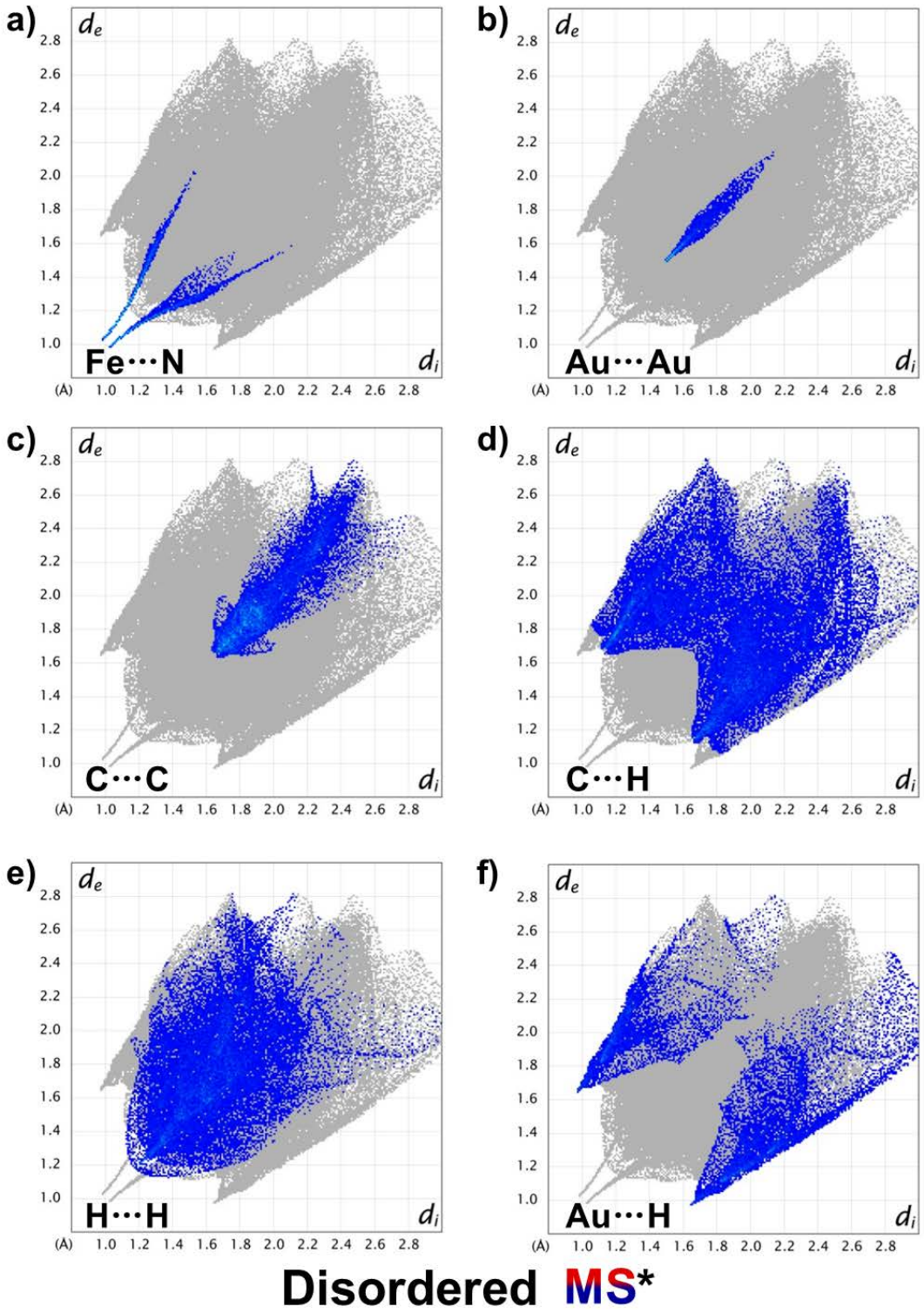

Figure S21. Fingerprint plot of **1** in the disordered MS* state at 80 K resolved into Fe...N (a), Au…Au (b), C…C (c), C…H (d) H…H (e) and Au…H (f) contacts. The full fingerprint is plotted beneath (grey).

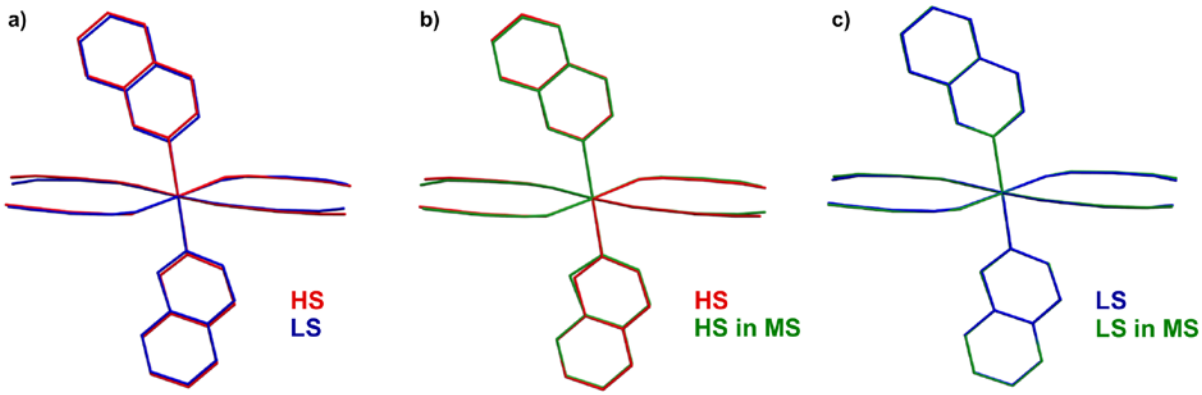

Figure S22 Overlapped crystal structure for **1** in the HS state at 170 K (red); in the ordered MS state at 80 K (green); and in the LS state at 80 K (blue).